SAND2013-7267C

Nano-Ordering of Donor-Acceptor Interactions Using Metal-Organic Frameworks as Scaffolds

Kirsty Leong,[1] Michael E. Foster,[1] Bryan M. Wong,[1] Erik D. Spoerke,[2] Dara Gough,[2] Joseph C. Deaton,[3] Mark D. Allendorf,[1*]

[1]Sandia National Laboratories, Livermore, CA 94551-0969
[2]Sandia National Laboratories, Albuquerque, NM 87185-1411
[3]Department of Chemistry, North Carolina State University, Raleigh, NC 27965

*e-mail: mdallen@sandia.gov

Metal-Organic Frameworks (MOFs) are nanoporous materials with tunable pore sizes that can accommodate and stabilize small molecules. Because of their long-range order and well-understood pore environment, the nano-confinement of donor-acceptor materials within MOFs offers a new methodology for creating uniform phase-segregated donor-acceptor interfaces. Phase segregation and the photo-physical effects of confining α,ω-Dihexylsexithiophene (DH-6T) and [6,6]-phenyl-C61-butyric acid methyl ester (PCBM) in several MOFs and the potential role of the MOF in creating a nano-heterojunction for organic photovoltaics are discussed. We demonstrate infiltration of both molecules into MOF pores and use luminescence and absorption spectroscopies to characterize the MOF-guest energy transfer processes. Comparison with density functional theory allows us to determine the energetics and band alignment within the MOF. The results demonstrate the utility of MOFs as scaffolds for sub-nanoscale ordering of donor and acceptor species within a highly uniform environment, allowing both the interaction and separation distance to be much more controlled than in the classical bulk heterojunction.

Introduction

The mechanism of charge separation in polymeric bulk hetero-junction photovoltaic cells is described as electron transfer from the absorbing polymer to an electron acceptor material. Two factors limiting the performance efficiency of OPV devices are the nature of the donor-acceptor (D-A) interface and the exciton diffusion length, which in conjugated polymers is typically < 10 nm before recombination occurs.[1] Much OPV research is directed toward ensuring that the D-A materials form continuous nanoscale networks within the entire photoactive layer, that their interfacial area is maximized, and that they have the proper orientation for efficient exciton splitting.[2-4] A nanoscale interpenetrating network with crystalline order of both constituents is therefore a desirable architecture for the active layer in photovoltaic devices.[5, 6] Unfortunately, control over both the intermolecular (D-A) and meso (exciton diffusion) length scales is

extremely difficult to achieve in conventional bulk heterojunctions due to the inherent disorder of polymeric and/or molecular species in a (typically) amorphous matrix

MOFs are a class of hybrid supramolecular materials formed from metal cations or clusters serving as "nodes" connected to multi-topic, electron-donating organic ligands, creating ordered networks with permanent nanoporosity.[7-9] MOFs possess three critical properties relevant to controlling donor-acceptor interfaces. First, they are crystalline materials, which create a highly ordered and well-defined structure in which the position of all framework atoms is known with sub-angstrom precision. Second, they incorporate both inorganic and organic components, providing an unprecedented ability to tune the electronic structure. This also enables the pore size and chemical environment to be tailored.[10-12] Third, the rigid MOF structure creates permanent nanoporosity. (1 – 10 nm diameter), which enables the fabrication of hybrid composites by filling the pores with guest molecules. This suggests that MOFs can serve as passive hosts to maintain close proximity and proper intermolecular alignment between donor and acceptor for efficient energy or charge transfer.

In this paper, the photo-physical effects of confining an electron donor, α,ω-Dihexylsexithiophene (DH-6T), and an electron acceptor, [6,6]-phenyl-C61-butyric acid methyl ester (PCBM), in several MOFs and the potential role of the MOF in creating a nano-heterojunction for organic photovoltaics will be discussed. We demonstrate infiltration of both molecules into MOF pores and use luminescence to characterize the MOF-guest energy transfer processes. Comparisons with density functional theory allow us to determine the energetics and band alignment within the MOF. These results demonstrate the utility of MOFs as scaffolds for sub-nanoscale ordering of donor and acceptor species, allowing both the interaction and separation distance to be much more controlled than in the classical bulk heterojunction.

Results and Discussion

Electronic structure calculations

Using first-principles electronic structure calculations, the band gap and band alignment of MOF-177 are such that neither energy nor charge transfer are feasible from infiltrated molecules to the framework. Based on self-consistent charge density-functional tight-binding (SCC-DFTB) calculations, the band gap of MOF-177 is predicted to be 3.55 eV, with a valence band (VB) maximum at -6.15 eV and conduction band (CB) minimum at -2.80 eV.

The partial density of states (PDOS) (Figure 1) indicates that the composition of the MOF-177 band edges is dominated by the H_3BTB linker, with minimal contribution from the zinc clusters (Zn-O). The MOF-177 excitation and emission maxima occur at 345 and 380 nm, respectively, whereas these maxima occur at 345 nm and 390 nm for H_3BTB in dilute solution (Figure 2). The slight (10 nm) blue shift in the MOF-177 emission spectrum is similar to what is observed in other Zn-carboxylate MOFs.[13]

(Guest molecule)@MOF-177. SCC-DFTB calculations show that MOF-177 can accommodate both DH-6T and PCBM and that infiltration is energetically favorable, both of which agree with experimental results described in the next section. Boltzmann

averages of the total energies created upon rotation are plotted versus the translational increments in (Figure 3).

DH-6T and PCBM Infiltration

Immersing MOF-177 crystals in saturated chlorobenzene solutions containing DH-6T, PCBM, and mixtures of the two molecules produces rapid, visually discernable color changes after a few hours of exposure. After one week, the translucent, colorless MOF crystals immersed in the DH-6T solution become pale yellow, while those exposed to PCBM become dark violet. PXRD of MOF-177 and infiltrated MOF-177 (Figure 4) show no changes to the framework or the presence of new phases, indicating that the framework maintains its integrity in the presence of DH-6T and PCBM.

Steady-state and time-resolved luminescence spectroscopy demonstrate that energy transfer occurs from the framework to DH-6T and PCBM guest molecules, whether they are present in the pores separately or as mixed components. The emission spectrum of DH-6T@MOF-177 exhibits quenching of the MOF's emission and the simultaneous appearance of a weak, broad emission band at lower energy (450-700 nm; Figure 5a). The weak emission band at lower energy corresponds to the emission of DH-6T. The infiltration of DH-6T into MOF-177 results in energy transfer from the MOF to DH-6T resulting in the emission of DH-6T at lower energy.

PCBM is an even more effective quencher of the MOF luminescence than DH-6T. The presence of PCBM in MOF-177 results in complete quenching of the MOF emission (Figure 5b). The presence of both DH-6T and PCBM in the MOF leads to an emission spectrum similar to PCBM@MOF-177.

Lifetime measurements show that dynamic quenching is responsible for the luminescent behavior observed in the infiltrated MOF-177. Steady-state lifetime measurements of MOF-177 and infiltrated MOF-177 were carried out, and the transient decay curves were fit to bi-exponential expressions for DH-6T@MOF-177 and PCBM@MOF-177 and a tri-exponential expression for DH6T+PCBM@MOF-177 tabulated in Table 1. The average lifetime (τ_{avg}) of the MOF-177 PL decreases upon infiltration with DH-6T, PCBM, and both DH-6T and PCBM, from 23 ns to 14 ns, 9 ns, and 6 ns, respectively. This decrease is consistent with dynamic quenching. The lifetime of DH6T+PCBM@MOF-177 is similar to PCBM@MOF-177, suggesting that PCBM plays a dominant role in the quenching process than DH-6T. The concentration and temperature dependence of the MOF-177 linker quenching by DH-6T and PCBM in solution is also consistent with dynamic quenching.

The luminescent quenching spectra along with concentration dependent study show energy transfer from the MOF to the guest molecules. The spectroscopic data presented here suggest Förster resonance energy transfer (FRET) is the dominant energy transfer mechanism in these (D+A)@MOF systems. Spectral overlap between the MOF-177 emission and DH-6T/PCBM absorbance is a requirement for efficient FRET to occur between emitting and absorbing molecules; this clearly exists for (DH-6T+PCBM)@MOF-177 (Figure 6).

Conclusions

The results just described demonstrate that MOFs can function as simultaneous hosts for organic donor and acceptor molecules typical of those used in excitonic devices such as bulk heterojunctions and solid-state lighting. Moreover, although by the nature of their constituents and bonding most MOFs are nominally insulators, even these can play an active role by interacting as a photon antenna to harvest light that is not efficiently absorbed by the donor. The results here show that by taking full advantage of the MOFs porosity as well as its structural order, one can create a MOF-donor-acceptor hybrid in which all constituents play an active role.

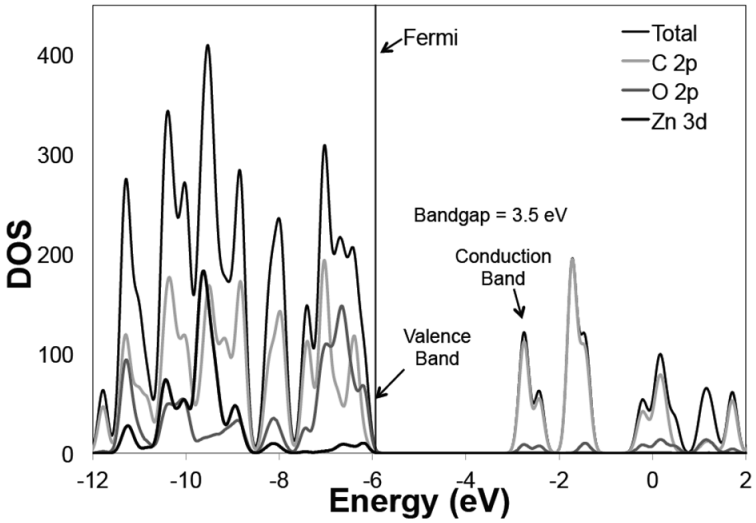

Figure 1. Partial Density of States (PSOD) - Tight-Binding Density Functional Theory (DFTB) of MOF-177.

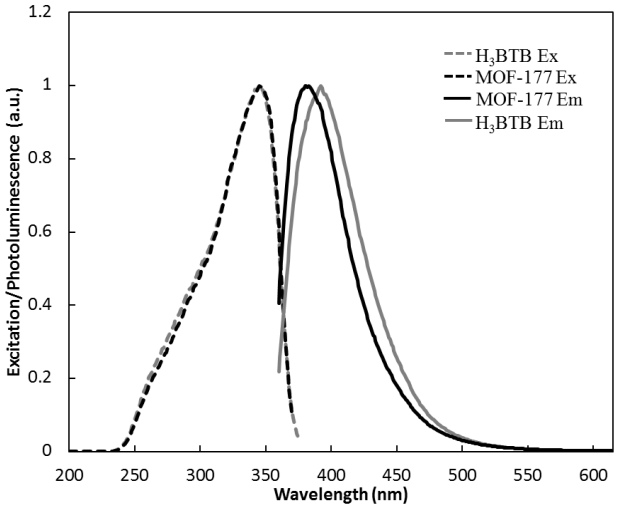

Figure 2**.** Solid state excitation and emission of MOF-177 and dilute solution of H_3BTB in DMF (1.0×10^{-6}M) . MOF-177: $\lambda(ex)_{max}$= 345 nm; $\lambda(em)_{max}$= 380 nm. H_3BTB: $\lambda(ex)_{max}$= 345 nm; $\lambda(em)_{max}$= 390 nm.

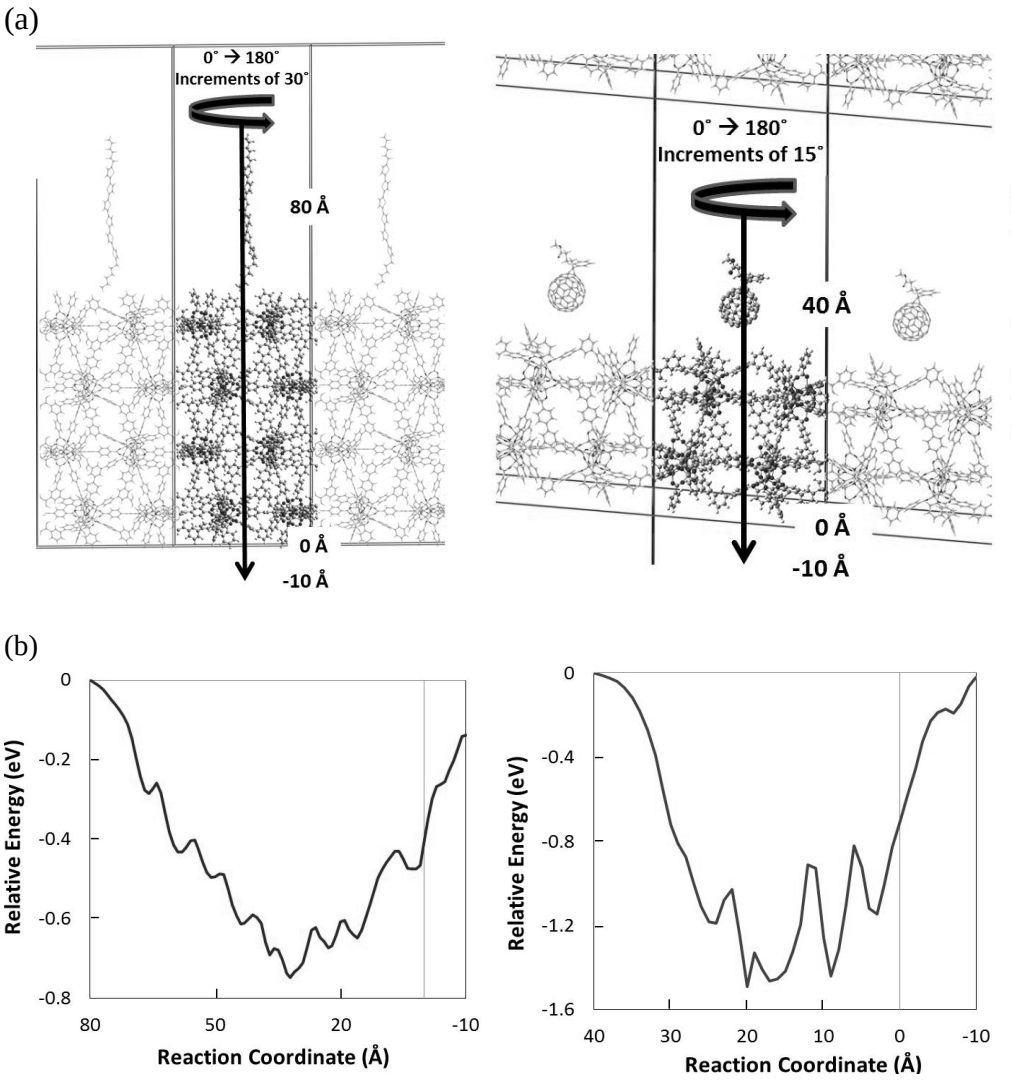

Figure 3**.** (a) Schematics showing the infiltration of MOF-177 with DH6T (left) and PCBM (right). (b) Potential energy curves of the infiltration process with DH-6T (left) and PCBM (right) determined at the SCC-DFTB level of theory. The reaction coordinate corresponds to the distance between the bottom of the unit cell and the center-of-mass of DH-6T or PCBM.

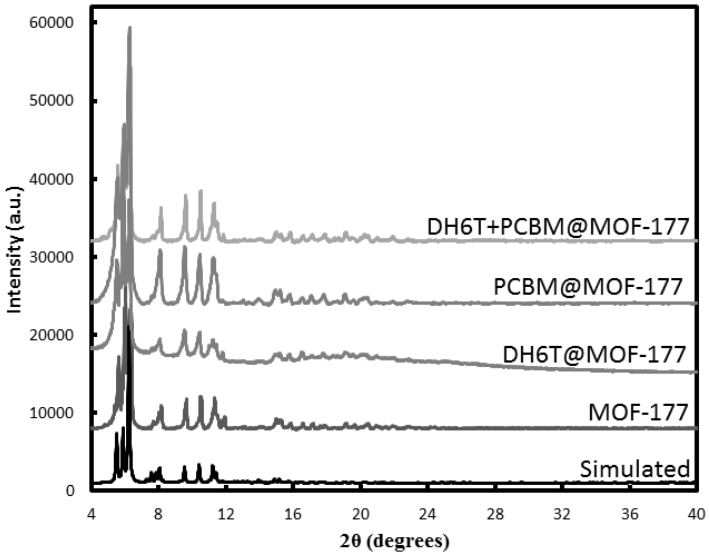

Figure 4**.** PXRD data for MOF-177 and infiltrated MOF-177.

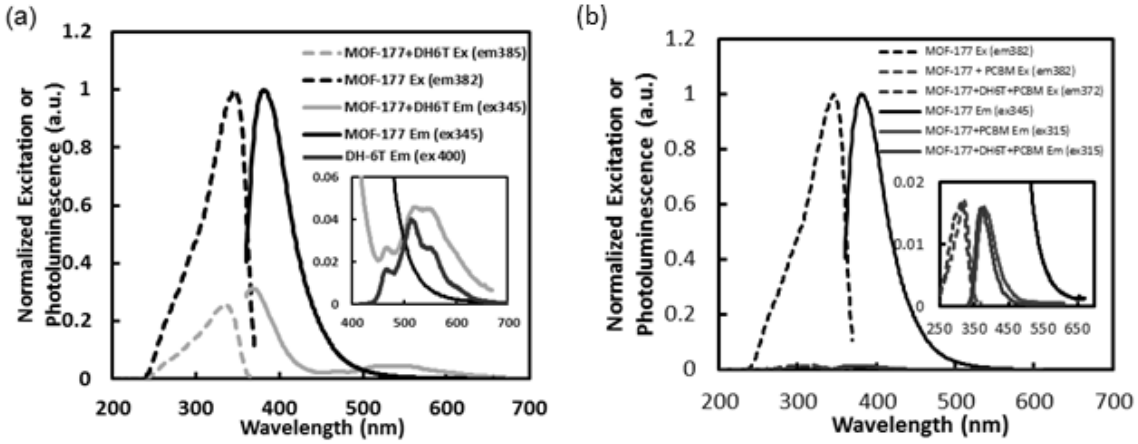

Figure 5. Photoluminescence spectra of (a) solid state MOF-177 and DH-6T@MOF-177; DH6T emission (insert) and (b) solid state MOF-177, PCBM@MOF-177, and DH6T+PCBM@MOF-177.

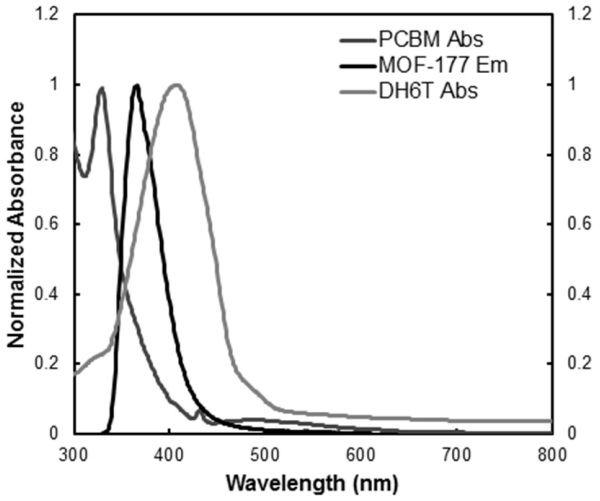

Figure 6**.** Spectral overlap of MOF-177 emission with DH6T and PCBM absorption.

TABLE I. Solid state lifetimes of MOF-177and infiltrated MOF-177.

	τ_0	τ_1	τ_2	τ_{avg}
MOF-177	10 (22%)	24 (78)	-	23
DH6T@MOF-177	8 (25%)	15 (75%)	-	14
PCBM@MOF-177	1 (22%)	9 (78%)	-	9
DH6T+PCBM@MOF-177	4 (6%)	15 (2%)	0.4 (92%)	6

Acknowledgments

This work was supported by the U.S. Department of Energy Office of Energy Efficiency and Renewable Energy SunShot Program under award number DE-FOA-0000387-1923 and Sandia National Laboratories' Laboratory Directed Research and Development (LDRD) Program. The authors are grateful to Prof. Jeffrey Long and Brian Weirs (UC Berkeley Dept. of Chemistry) use of their UV-Vis/diffuse reflectance instrument. Sandia National Laboratories is a multi-program laboratory managed and operated by Sandia Corporation, a wholly owned subsidiary of Lockheed Martin Corporation, for the U.S. Department of Energy's National Nuclear Security Administration under contract DE-AC04-94AL85000.

References

1. T. Kirchartz, K. Taretto and U. Rau, *The Journal of Physical Chemistry C* **113** (41), 17958-17966 (2009).
2. W. U. Huynh, J. J. Dittmer and A. P. Alivisatos, *Science* **295** (5564), 2425-2427 (2002).
3. S. E. Shaheen, C. J. Brabec, N. S. Sariciftci, F. Padinger, T. Fromherz and J. C. Hummelen, *Applied Physics Letters* **78** (6), 841-843 (2001).
4. M. M. Wienk, J. M. Kroon, W. J. H. Verhees, J. Knol, J. C. Hummelen, P. A. van Hal and R. A. J. Janssen, *Angewandte Chemie International* Edition **42** (29), 3371-3375 (2003).
5. P. Peumans, S. Uchida and S. R. Forrest, *Nature* **425** (6954), 158-162 (2003).

6. L. Schmidt-Mende, A. Fechtenkötter, K. Müllen, E. Moons, R. H. Friend and J. D. MacKenzie, *Science* **293** (5532), 1119-1122 (2001).
7. G. Ferey, *Chemical Society Reviews* **37** (1), 191-214 (2008).
8. H. Li, M. Eddaoudi, M. O'Keeffe and O. M. Yaghi, *Nature* **402** (6759), 276-279 (1999).
9. J.-R. Li, R. J. Kuppler and H.-C. Zhou, *Chemical Society Reviews* **38** (5), 1477-1504 (2009).
10. R. Banerjee, H. Furukawa, D. Britt, C. Knobler, M. O'Keeffe and O. M. Yaghi, *Journal of the American Chemical Society* **131** (11), 3875-3877 (2009).
11. Y. Cui, Y. Yue, G. Qian and B. Chen, *Chemical Reviews* **112** (2), 1126-1162 (2011).
12. M. Eddaoudi, J. Kim, N. Rosi, D. Vodak, J. Wachter, M. O'Keeffe and O. M. Yaghi, *Science* **295** (5554), 469-472 (2002).
13. J. J. Perry IV, P. L. Feng, S. T. Meek, K. Leong, F. P. Doty and M. D. Allendorf, *Journal of Materials Chemistry* **22** (20), 10235-10248 (2012).